High pressure study of ZnSe:Cr^{2+} crystals: the origin of the 1.25 eV luminescence

High pressure study of ZnSe:Cr^{2+} crystals: the origin of the 1.25 eV luminescence

S Trushkin, S W Biernacki, Le Van Khoi and A Suchocki

Institute of Physics, Polish Academy of Sciences, Aleja Lotników 32/46, 02-668 Warsaw, Poland

Abstract
High pressure studies of Cr^{2+} luminescence in ZnSe crystals were performed at low temperatures. In addition to the mid-infrared luminescence transitions from the first excited ^{5}E level, higher energy luminescence was also observed. These two luminescence bands exhibit similar pressure coefficients but of opposite signs, which identify the origin of the higher energy band as the transitions from the second excited ^{3}T$_1$ level. At higher pressures, increased covalence effects are observed, which result in the appearance of an additional peak in the ^{5}E $\rightarrow$ ^{5}T$_2$ luminescence due to changes in the spin–orbit coupling strength.

1. Introduction

The Cr^{2+} ion is a well known optically active centre in II–VI compounds. A mid-infrared lasing action was reported for Cr^{2+}-doped ZnS, ZnSe and CdMnTe [1–3], as well as the construction of a broadly tunable, room-temperature, continuous-wave laser near 2.5 μm [4]. Such mid-infrared coherent sources are supposed to be essential in various medical applications, inasmuch as any biological tissue has an absorption maximum around 2.9 μm [5]. Besides, low concentrations of pollutant gas molecules could be easily detected using the above mentioned laser systems, which makes them especially attractive for environmental diagnostics and the coal-mining industry. Recently, II–VI Cr-doped semiconductors also captured researchers' attention as prospective materials for spintronics [6–9].

The ZnSe:Cr crystals exhibit at low temperatures two broad infrared photoluminescence bands with peaks at about 0.52 and 1.25 eV [10]. The first photoluminescence band is associated with the Cr^{2+} ^{5}E $\rightarrow$ ^{5}T$_2$ intra-shell transition [1, 11, 12]. The second near-infrared emission was also observed in ZnS:Cr crystals [13]. Its nature is not yet identified and it was widely discussed in the literature. This photoluminescence (PL) band has previously been assigned to the ^{4}T$_1$ $\rightarrow$ ^{6}A$_1$ transition of Cr$^+$ [14] and later it has been interpreted in terms of a ^{3}T$_1$ $\rightarrow$ ^{5}T$_2$ transition within the d^4 configuration of Cr^{2+} [15, 10]. In order to clarify this issue we applied high pressure, low temperature spectroscopy with use of a diamond-anvil cell (DAC), which is a very powerful tool in material science research for identification of the energy structure of various dopant ions [16, 17].

2. Experimental details

High pressure measurements were performed using a Diacell Products MCDAC-1 diamond–anvil cell. Argon was applied as a pressure-transmitting medium. The diamond-anvil cell was mounted in an Oxford 1204 cryostat equipped with a temperature controller for low temperature measurements. The R_1 ruby luminescence line was used as a reference pressure sensor. The polished single-crystalline samples about 30 μm thick were loaded into the cell along with a small piece of ruby. The emission spectra were excited by the 514.5 and 488 nm argon-ion laser lines and measured with the use of an MDR-2 monochromator equipped with a Hamamatsu (P819) solid CO_2-cooled PbS detector and a 7265 DSP EG&G Instruments lock-in amplifier. The spectra were corrected for the quantum efficiency of the system. To measure the luminescence the argon-ion laser line was focused either on the measured ZnSe:Cr sample or on the ruby. The pressure calibration with use of ruby luminescence was performed at low temperature. However, the pressure was changed at room temperature in order to minimize non-hydrostatic effects that are known to exist in diamond-anvil cells, especially at higher pressures. The hydrostatic conditions could be partially monitored by recording the half-width of the ruby emission. In our measurements, we observed an increase of the half-width of ruby luminescence with pressure growth. However, the half-width of the R_1 ruby luminescence did not exceed 5 cm^{-1} at high pressures (2.5 cm^{-1} at ambient pressure; 1 meV = 8.065 cm^{-1}). This means that the non-hydrostatic effects were rather weak.

3. Experimental results and discussion

Numerous studies of the free Cr^{2+} ion terms and the crystal-field (CF) terms in II–VI compounds reveal noticeable disagreement between the calculated and experimental energy terms [18–22]. Consideration of the Trees correction, the spin polarization due to the Coulomb exchange energy in the partly filled 3d electronic shell [23, 24], and the covalence effects [25, 26] improves the general agreement between theory and experiment; however, details of the CF term structure are still not clear. Generally, the agreement between calculations and observations for the neighbouring configurations d^3 of the V^{2+} ion and d^5 of the Mn^{2+} ion is remarkably better than for the d^4 configuration of Cr^{2+}.

The general difficulty in the understanding of the structure of Cr^{2+} CF terms compelled us to study again the ZnSe:Cr luminescence as a function of applied hydrostatic pressure. Two luminescence bands centred on 0.6 and 1.25 eV were investigated within the 0–80 kbar pressure range. The 0.6 eV band shown in figure 1 evidently belongs to the ^{5}E $\rightarrow$ ^{5}T$_2$ transition. The optical transitions between these terms were investigated by Kaminska *et al* [20]. A variation of the d-orbital energy of JT distorted T_d complexes was also studied by Valiente and Rodriguez [27]. Both terms exhibit the Jahn–Teller (JT) effect and the value of JT energy ε_{JT} was extracted from the line shape fit to observed spectra. Moreover, a comparison of the Cr^{2+} spectra in ZnS, ZnSe and CdTe indicates that in ZnSe the spin–orbit splitting of the ^{5}T$_2$ term is negligible. This was explained by the particular ratio of the admixture of the ligand p function to the d function. The deduced JT energy of the ^{5}T$_2$ ground state is $\varepsilon_{JT}(^5T_2) = 340$ cm^{-1} and a much smaller JT interaction in the excited ^{5}E state, $\varepsilon_{JT}(^5E) = 40$ cm^{-1}, was found [20]. More detailed inspection of figure 1 shows that at higher pressure an additional band appears at the low energy side of the spectrum. At 82 kbar, this extra band peaks at an energy of about 0.58 eV, in addition to two other peaks at 0.62 and 0.68 eV. The pressure dependence of the 1.25 eV band is shown in figure 2.

Figure 3 shows pressure dependences of the spectral positions of the Cr^{2+} luminescence maxima in the ZnSe:Cr crystal at low temperatures. From this graph it follows that the
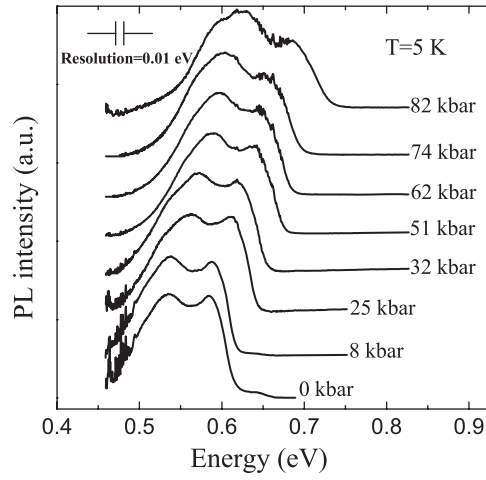
2

Figure 1. Pressure dependence of the 0.6 eV Cr^{2+} luminescence band of the ZnSe:Cr crystal at $T = 5$ K.
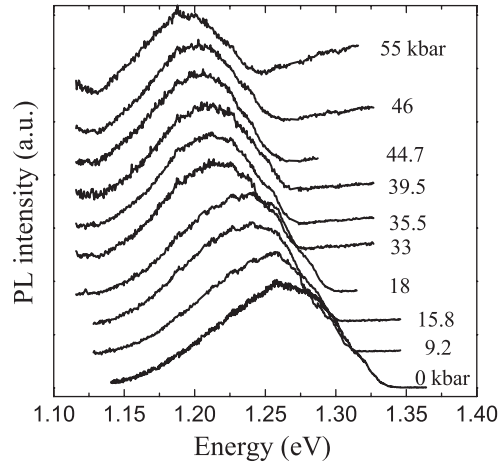

Figure 2. Pressure dependence of the 1.25 eV luminescence band of the ZnSe:Cr crystal at $T = 10$ K.

energy maxima of the 0.6 eV band split by the Jahn–Teller effect increase nearly linearly with increasing pressure. The pressure coefficients of these maxima are similar and equal to about 8 cm^{-1} $kbar^{-1}$.

In a standard CF point charge model the $^5E \rightarrow {}^5T_2$ transition energy depends only on the cubic CF parameter Δ and it is given as [25] (CGS units)

$$\Delta = 10Dq = \frac{10}{6}Z\frac{e^2\langle r^4\rangle}{R^5} \tag{1}$$

where R is the interatomic distance Cr–Se approximated by the Zn–Se separation, $\langle r^n\rangle = \int R_{3d}r^{n+2}\,dr$, and Ze is the charge of the ligand ion. Hydrostatic pressure reduces the distance R and then Δ can be scaled from the value for ambient pressure using the Murnaghan scaling
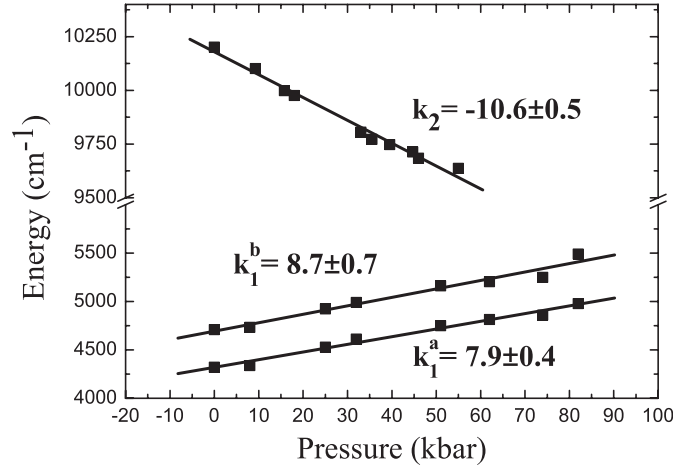
Figure 3. Pressure dependences of the spectral position of the Cr^{2+} luminescence maxima in the ZnSe:Cr crystal at low temperatures. The pressure coefficients k of the peaks of the luminescence bands are given in the graph in units of cm^{-1} $kbar^{-1}$.
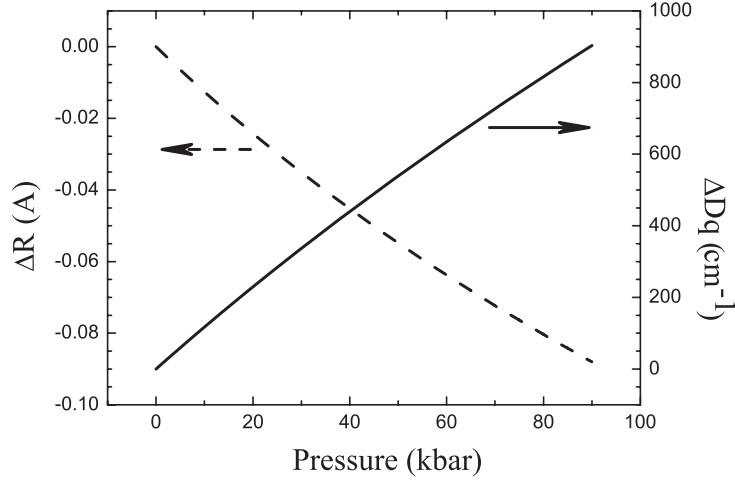

Figure 4. The calculated changes of R and Dq with pressure.

factor [28]:

$$\frac{R_0}{R_p} = \left(\frac{pB'_0}{B_0} + 1 \right)^{1/3B'_0} \tag{2}$$

where $B_0 = 624$ kbar is the bulk modulus and $B'_0 = 4.77$ is its pressure derivative for the ZnSe crystal [29, 30]. The calculated pressure dependences of changes of interatomic distance ΔR and changes of the cubic CF strength parameter ΔDq are shown in figure 4.

The change of Dq is slightly bow shaped. Further on, we approximate this dependence as linear. Therefore, as seen from figure 4, the pressure coefficient of Dq is close to 8 cm^{-1} $kbar^{-1}$, which is in a good agreement with the pressure coefficients of two components of the 0.6 eV band.
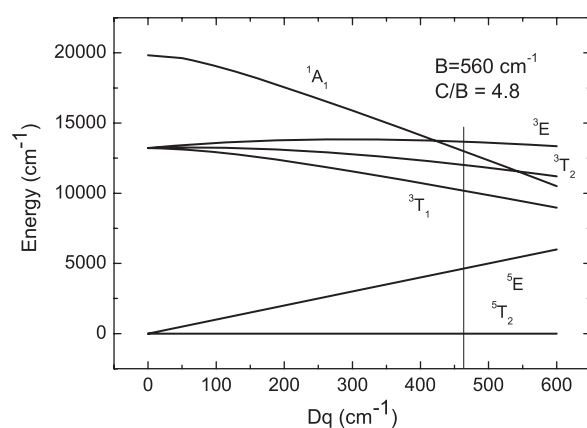
4

Figure 5. The Tanabe–Sugano diagram for the six lowest CF terms of the d^4 configuration in a tetrahedral crystal field.

The transition between the ground and the first excited term is accompanied by the conversion of one e electron by the energy $10Dq$. The conventional Tanabe–Sugano diagrams [25] show the CF term energies for a particular value of the crystal-field strength parameter Dq. The Tanabe–Sugano diagram for the six lowest CF terms of the d^4 electronic configuration in a tetrahedral CF is shown in figure 5.

The 0.6 eV luminescence bands correspond to the transition from the ^5E to $^5T_2$ term. The energy surface of the ^5E term has the form of a 'Mexican hat'. The ground sub-levels of the $^5T_2$ term are split. This splitting is determined by the equilibrium position of the ^5E term on the coordinate configuration diagram. Since the estimation based on the CF theory suggests different tetragonal coupling constants for both terms the observed energy distance of 380 cm^{-1} is not equal to the splitting $3E_{JT}$ of the $^5T_2$ term at its equilibrium deformation. The energy $3E_{JT}$ obtained from the direct absorption between sub-levels of the $^5T_2$ term is three to four times larger. The ligand displacement from the equilibrium position is proportional to the electron–lattice coupling constant while the JT splitting to the square of this constant. Taking this into account we find that the equilibrium displacement of the ligands for the ^5E term is approximately equal to half of that for the $^5T_2$ term.

The luminescence shows broadening not only due to rotation about the tetragonal axis for the ^5E term but also due to the breathing vibration around the equilibrium position, that directly influences $10Dq$. The amplitude of such vibration can be estimated from the relation $kQ_b^2 \approx h\omega$. Taking $h\omega = 300 \text{ cm}^{-1}$, one obtains that the maximal amplitude is $\Delta R \sim 0.05$ Å. Therefore, the total shift for inside and outside motion around the equilibrium is ~ 0.1 Å. As shown in figure 4, the shift of $\Delta R \approx 0.05$ Å is equivalent to application of 50 kbar pressure. The corresponding shift in the value of $\Delta 10Dq$ is about 500 cm^{-1}. Thus, the thermal vibration of ligands around their equilibrium causes harmonic oscillation in the average value of $10Dq$ of $\approx 500 \text{ cm}^{-1}$.

Hydrostatic compression leads to a decrease of R and hence an increase of cubic CF. This is clearly seen in figures 1 and 3, where both peaks of the 0.6 eV emission show positive pressure coefficients equal to about $8 \text{ cm}^{-1} \text{ kbar}^{-1}$. Of course, hydrostatic pressure does not change the site symmetry of the centre but it can change the amplitude of tetragonal distortion.

A more accurate description of the $^5E \leftrightarrow {}^5T_2$ optical transitions of Cr^{2+} ions in II–VI compounds requires taking into account both Jahn–Teller and spin–orbit interactions [20].

Accidentally, at ambient pressure the spin–orbit interaction parameter $\lambda = 0$ for ZnSe:Cr^{2+}; however, this parameter is not equal to zero for the other II–VI compounds, which results in the splitting of the $^5E \rightarrow {}^5T_2$ luminescence band into three sub-bands, instead of the two sub-bands observed for ambient pressure ZnSe:Cr. The appearance of the additional band with increased pressure can be explained by the pressure induced admixture of ligand wavefunctions into the central ion wavefunctions (the nephelauxetic effect) [31]. It is known that even a small admixture of the ligand wavefunctions may have a significant influence on the spin–orbit parameter [20]. The nephelauxetic effect obviously increases with applied pressure [32], and changes the value of the spin–orbit parameter, which explains the appearance of the additional band in the $^5E \rightarrow {}^5T_2$ luminescence spectrum and changes in the intensities of the sub-bands.

The pressure coefficient of the 1.25 eV luminescence band is negative and its absolute value is similar to that of the 0.6 eV band. The 1.25 eV band is broader and does not exhibit any splitting, in contrast to the 0.6 eV band. The low temperature luminescence measurements at ambient pressure of a bulk ($\sim$1 mm thick) ZnSe:Cr sample also reveal the zero-phonon line of this band located around 1.32 eV. This line cannot be observed in our experimental set-up. The very thin samples used in the experiment and, consequently, low intensity of emission in DAC limits the spectral resolution of our data. The Tanabe–Sugano diagram indicates that the $^3T_1 \rightarrow {}^5T_2$ transition is the most probable candidate for the origin of this band. The $^3T_1$ state is the second excited state of the Cr^{2+} ion in a tetrahedral CF. The relatively large energy of this transition and the relatively large energetic distance from the first excited ^5E state makes the radiative transitions from this level quite probable.

There are a few $^3T_2$ and $^3T_1$ terms within the d^4 configuration. The two lowest terms shown in figure 5 consist mainly (about 90%) of the t_2e^3 configuration. Therefore, both terms should undergo tetragonal distortion and the transition from these terms to the ground $^5T_2$ level should show splitting. However, in both terms the e^3 electrons are shared in a different manner among the $d_v = v$ and $d_u = u$ orbitals and this makes the essential difference in their behaviour. We shall illustrate this in detail. The diagonal matrix elements of tetragonal distortion (elongation or contraction along the z axis) for the d states are $\langle xz \parallel xz \rangle = \langle yz \parallel yz \rangle = V/7$, $\langle xy \parallel xy \rangle = -2V/7$, $\langle u \parallel u \rangle = 2V/7$, and $\langle v \parallel v \rangle = -2V/7$. Here $\parallel$ denotes the corresponding operator of tetragonal distortion and V is the JT coupling constant. The z components of the wavefunction in the form of the Slater determinant of the term under consideration are [25] $|{}^3T_{1Z}\rangle = |xy, u, \underline{u}, v\rangle$ and $|{}^3T_{2z}\rangle = |xy, u, v, \underline{v}\rangle$, where the opposite spin orientation is underlined. The tetragonal distortion for the considered components is $\langle {}^3T_{1Z} \parallel {}^3T_{1Z}\rangle = (-2/7+2/7+2/7-2/7)V = 0$ and $\langle {}^3T_{2Z} \parallel {}^3T_{2Z}\rangle = (-2/7+2/7-2/7-2/7)V = -4V/7$. Therefore, within this approximation the $^3T_1$ term is not JT active while the $^3T_2$ term shows strong distortion. Since the final term for the luminescence starting from the non-distorted $^3T_1$ term is also free of distortion, we conclude that the 1.25 eV luminescence is the $^3T_1$–$^5T_2$ transition. Of course, $^3T_1$ consists of around 10% of other electron configurations (six of a total of seven), which produces some residual distortion. However, the $^3T_1$–$^5T_2$ transition is rather strongly crystal field dependent and the expected splitting is hidden in the thermal width of the luminescence line. The two excited terms involved in luminescence also show different breathing distortions. Taking the $^5T_2$ term with the configuration $t_2^2e^2$ as reference equilibrium for the ligand tetrahedron, the term ^5E with the configuration t_2^3e produces enlargement of the tetrahedron while the term $^3T_1$ with configuration t_2e^3 produces its contraction. This means, contrary to the Tanabe–Sugano diagrams, little difference in Dq for both transition lines and, additionally, a different portion of the Coulomb repulsion energy in the transition. The latter comes from the different degree of covalence (the admixture of the ligand functions to the 3d functions—again the nephelauxetic effect) in each term separated by quite large energy intervals. Thus, the energy difference between ^5E and $^5T_2$ is not pure $10Dq$ energy. This, at

least partly, explains some small difference in the absolute values of the pressure coefficients for the 1.25 and 0.65 eV lines. Although the luminescence between the $^3T_1$ and $^5T_2$ can be easily detected, the spin-forbidden character of the $^3T_1 \leftrightarrow {}^5T_2$ transitions makes them difficult to observe in the absorption spectra.

One can speculate that the 1.25 eV band is due to the Cr^{1+} charge state. The $Cr^{2+} \rightarrow Cr^{1+}$ photo-transformation process upon illumination of the crystal by the argon ion laser light was reported in ZnSe:Cr crystals in [33]. The possible candidate for this would be the $^4T_1 \rightarrow {}^6A_1$ transition within the d^5 electronic configuration of the Cr^{1+} ion. However, such a transition should be observed at much higher energy, according to Tanabe–Sugano diagrams for the d^5 configuration (calculated also with the parameters for Cr^{2+}) [34]. Hence, we assume that both luminescence bands belong to the Cr^{2+} charge state.

4. Conclusions

In summary, the high-pressure luminescence measurements at low temperature unambiguously indicate that the 1.25 eV luminescence band in ZnSe:Cr is associated with the intrashell $^3T_1 \rightarrow {}^5T_2$ transitions of the Cr^{2+} ion. The increased admixture of the ligand wavefunctions into the central ion wavefunctions with applied pressure has been found responsible for the changes in the value of the spin–orbit parameter and appearance of the additional band in the $^5E \rightarrow {}^5T_2$ luminescence spectra at higher pressures.

Acknowledgment

References

[1] DeLoach L D, Page R H, Wilke G D, Payne S A and Krupke W F 1996 *IEEE J. Quantum Electron.* **32** 885
[2] Page R H, Schaffers K I, DeLoach L D, Wilke G D, Patel F D, Tassano J B, Payne S A, Krupke W F, Chen K-T and Burger A 1997 *IEEE J. Quantum Electron.* **33** 609
[3] Hommerich U, Wu X, Davis V R, Trivedi S B, Grasza K, Chen R J and Kutcher S 1997 *Opt. Lett.* **22** 1180
[4] Sorokin E and Sorokina I T 2002 *Appl. Phys. Lett.* **80** 3289
[5] Sorokina I T 2004 *Opt. Mater.* **26** 395
[6] Katayama-Yoshida H and Sato K 2003 *J. Phys. Chem. Solids* **64** 1447
[7] Saito H, Zayets V, Yamagata S and Ando K 2003 *Phys. Rev. Lett.* **90** 207202
[8] Saito H, Zayets V, Yamagata S and Ando K 2003 *J. Appl. Phys.* **93** 6796
[9] Kulatov E, Uspenskii Y, Mariette H, Cibert J, Ferrand D, Nakayama H and Ohta H 2003 *J. Supercond.* **16** 123
[10] Ivanov V Yu, Shagov A A, Szczerbakow A and Godlewski M 2001 *Physica* B **308–310** 942
[11] Grebe G, Roussos G and Schulz H-J 1976 *J. Lumin.* **12/13** 701
[12] Grebe G, Roussos G and Schulz H-J 1976 *J. Phys. C: Solid State Phys.* **9** 4511
[13] Grebe G and Shulz H-J 1974 *Z. Naturf.* a **29** 1803
[14] Pradella H and Pohl U W 1987 *Phys. Status Solidi* b **141** K143
[15] Lehr M U, Litzenburger B, Kreissl J, Pohl U W, Selber H R, Schulz H-J, Klimakow A and Worschech L 1997 *J. Phys.: Condens. Matter* **9** 753
[16] Kamińska A, Kaczor P, Durygin A, Suchocki A and Grinberg M 2002 *Phys. Rev.* B **65** 104106
[17] Galanciak D, Grinberg M, Gryk W, Kobyakov S, Suchocki A, Boulon G and Brenier A 2005 *J. Phys.: Condens. Matter* **17** 7185
[18] Vallin J T, Slack G A, Roberts S and Hughes A E 1970 *Phys. Rev.* B **2** 4313
[19] Nygren B, Vallin J T and Slack G A 1972 *Solid State Commun.* **11** 35
[20] Kaminska M, Baranowski J M, Uba S M and Vallin J T 1979 *J. Phys. C: Solid State Phys.* **12** 2197
[21] Griffith J S 1961 *The Theory of Transition-Metal Ions* (Cambridge: Cambridge University Press)

[22]　Biernacki S and Schulz H-J 1987 *Z. Phys.* B **65** 429
[23]　Slater J C 1968 *Phys. Rev.* **165** 655
　　　Slater J C 1968 *Phys. Rev.* **165** 658
[24]　Hemstreet L A and Dimmock J O 1979 *Phys. Rev.* B **20** 1527
[25]　Sugano S, Tanabe Y and Kamimura H 1970 *Multiplets of Transiton Metal Ions in Crystals* (New York: Academic)
[26]　Fazzio A, Caldas M J and Zunger A 1984 *Phys. Rev.* B **30** 3430
[27]　Valiente R and Rodriguez F 1998 *J. Phys.: Condens. Matter* **10** 9525
[28]　Murnaghan F D 1944 *Proc. Natl Acad. Sci.* **30** 244
[29]　Rabah M, Abbar B, Al-Douri Y, Bouhafs B and Sahraoui B 2003 *Mater. Sci. Eng.* B **100** 163
[30]　Greene R G, Luo H and Ruoff A L 1995 *J. Phys. Chem. Solids* **56** 521
[31]　Jorgensen C K 1962 *Prog. Inorg. Chem.* **4** 73
[32]　Biernacki S W, Kamińska A, Suchocki A and Arizmendi L 2002 *Appl. Phys. Lett.* **81** 442
[33]　Światek K, Godlewski M and Surkova T P 2004 *Phys. Status Solidi* c **1** 281
[34]　Mahofer K, Hochberger K and Gebhardt W 1988 *J. Phys. C: Solid State Phys.* **21** 4393